CHARACTERIZATION OF THE MICROSTRUCTURE OF RANDOMLY-GENERATED PARTICLE PACKS FOR DEM SIMULATIONS OF GRANULAR MATERIALS

Kamila R. C. Seko

Eduardo M. B. Campello

kamilacassares@usp.br

campello@usp.br

Department of Structural and Geotechnical Engineering, University of São Paulo

P.O. Box 61548, 05424-970, São Paulo, SP, Brazil

Abstract. *In this work we generate packs of particles using the recently proposed particle-packing technique of Campello and Cassares and perform assessment of the microstructure of these packs. We compute each pack´s coordination number, fabric tensor, normal contact force tensor and tangential friction force tensor, such that the microstructure of the packs is fully characterized with respect to their granular fabric and principal contact directions (both normal and tangential). These quantities provide a good estimate to the degree of isotropy or anisotropy of the packs, and thus serve as indicators of "quality" of the packs and, ultimately, of our particle-packing technique. We show that the technique, besides being able to generate packs at sufficiently high packing ratios, is also able to generate packs that are very much repeatable with respect to their microstructure. This feature is extremely desirable if the packs are intended to serve as samples of granular materials on which DEM simulations are to be conducted, e.g. for material characterization purposes and/or determination of bulk material responses. This is indeed our interest in the next step of this research. We believe that simple, reliable techniques for generation of particle packs at sufficiently high packing ratios and with adequate microstructure are crucial tools for the DEM simulation of granular materials.*

Keywords: *Particle packing, Microstructure, Fabric system, Granular materials, Discrete element method.*

1 INTRODUCTION

Generally, behavior of engineering materials is written in terms of macroscopic characteristics. These characteristics are based on continuum parameters, such as stress and strain. Establishing stress-strain relationships to solve boundary value problems and determine a constitutive model to represent the physics of material behaviour are substantial for engineering interest. These techniques are as important as physical understanding through the treatment of a granular material as an assembly of interacting particles (with contact forces, contact orientations and microscopic parameters).

The mechanical behavior of granular materials can be studied to a good extent by the fabric (microstructure) and distribution of contact forces. Chang et al. in 1985, Darbre and Wolf in 1985, Rothenburg and Bathurst in 1989 and Emeriault and Cambou in 1996 are some researchers that proposed analytical constitutive models for granular materials composed of spheres with an assumed fabric (Ng, 1999).

Micromechanics study of granular assemblies can be performed by numerical or/and experimental techniques. These latter, however, are usually time consuming and sometimes subjective. Additionally, it is hard to produce identical specimens with which statistical analysis of results can be performed. Thornton and Barnes in 1986 highlighted the possibility of visual analysis of the internal deformation processes. For these reasons, in this work we choose numerical techniques to do it; specifically, we adopt the Discrete Element Method (DEM).

Some works using DEM simulation of plane assemblies of discs are: Cundall and Strack (1979); Cundall et al. (1982); Thornton and Barnes (1986); Bathurst and Rothenburg (1988); Rothenburg and Kruyt (2004); Kruyt (2012). These are regarded as already classical works on the field. Ng (1999) studied the fabric of granular materials after compaction. For three-dimensional assemblies of spheres, important contributions are: Darbre and Wolf (1985); Emeriault & Cambou (1996); Thornton and Antony (1998); Ng (1999); Thornton (2000); Ng(2001); Ng(2004). The search of Emeriault and Cambou, in 1996, emphasized the importance of micromechanical approach in modelling anisotropic elastic behaviour of granular materials and your applicability in soil analysis submitted to vibrations or very small amplitude cycles.

A discrete element method can be defined as a simulation method wherein the finite displacements and rotations of discrete bodies or particles are simulated. Throughout their motion, particles come into contact with each other and may lose the contact too. These changes have to be determined. However, the specification of the initial conditions and the boundary conditions are extremely important.

The response of a pack of particles or granular pack is intrinsically dependent on its initial state like packing density and stress level, the anisotropy of its fabric, the anisotropy of the stress state and the orientation of the principal stress relative to the fabric.

In this work, the technique applied to generate the particles packs is the one developed by Campello and Cassares in 2015. This technique, and the way that we will perform assessment of the microstructure of these packs, are shown below. We also show the calculation routine adopted to study the fabric of the packs.

2 RAPID GENERATION OF PARTICLES PACKS

We describe briefly the recently prosed particle-packing technique below (Campello; Cassares, 2015). We consider this procedure as simple and fast for generating particle packs at high packing ratios. Our technique consists in a generation of packs in a layer-by-layer fashion beginning from the bottom of the bulk domain until a desired total height is achieved. The bulk domain is defined a priori. We choose a rectangle for 2D packs and a prism for 3D packs. The positions of the particles in each new layer are treated as random variables whose values are sampled from underlying probability distribution functions (pdfs), following a random sequence addition (RSA) approach. After that a jamming force is activated and the motion reached by the particles is resolved through a DEM simulation. As consequence, the new layer settles down and interacts with the previous layer by mechanical contact. This procedure is repeated for new layers until the desired total height for the jammed pack is achieved.

The radii of the generated particles can either be the same for all particles or be sampled from ad-hoc pdfs. In this study, we choose a Gaussian distributions (mean value and standard deviation must be provided). It is necessary to highlight that we do not adopt a particle growth scheme in the jamming stage of our technique.

It is essential to control four aspects for the technique to attain density effectiveness and computational efficiency. They are: (1) the use of appropriate material parameters for the particles within the DEM simulations, so that the contacts and collisions due to the jamming forces result inelastic enough (it enforces the system to settle down very rapidly for each new layer and avoiding undesired bouncing of particles as well as high frequency motions, which would require small time steps to be resolved adequately); (2) the use of explicit time integration scheme to perform the DEM simulations (this improves computational efficiency); (3) the start of each new layer at moderate initial densities like $\bar{\phi} = 0.4$ in 2D pack and $\bar{\phi} = 0.25$ in 3D pack (this feature is inherited from the RSA algorithm); and (4) consideration of rotational motion with particle spin and inter-particle friction in the DEM simulations.

The technique can be implemented into a script code. It is summarized in the Algorithm 1 below.

Algorithm 1. Generation of particle packs

```
1.    Get bulk boundaries and domain data (shape and sizes)
2.    Get layers' properties (initial shape and sizes, initial density φ̄, particle size
      or particle size distribution, particles' material properties)
3.    Get desired height for the jammed pack
4.    Get jamming force data
5.    Get time integration data (time step size, simulation times)
6.    FOR i = 1,...,n_S (n_S = number of sets be generated) DO:
         FOR j = 1,...,n_P (n_P = number of packs in each set) DO:
            current height = 0
            WHILE (current height < desired height) DO
               Generate new layer on top of previous layer(s) via RSA
               Apply jamming force and run DEM simulation
               Compute current height
            END DO
         END DO
      END DO
```

3 MICROMECHANICS OF GRANULAR MATERIALS

DEM simulation is able to capture detailed information on the internal structure of a granular material in any point. The coordination number Z, for example, furnishes the average number of contacts per particle in the assembly. Using this result, we could measure the packing density. The definition of coordination number is

$$Z = 2\frac{N_c}{N_p}, \tag{1}$$

where N_c is the total number of physical contacts and N_p is the number of particles in the system. It is necessary to highlight that Z does not give us any information about orientations of interparticle contacts, contact forces magnitudes, shape and particles size. However, some researchers show that coordination number is related to pack density or void ratio.

The fabric tensor is a measure of changes in the fabric of granular materials. In addition, this tensor can be considered a measure of stress in a sample characterized by an induced anisotropy in contact normal orientations. The fabric tensor $\boldsymbol{R}$ is given as

$$R_{ij} = \frac{1}{2N_c}\sum_{c=1}^{N_c} n_i^c n_j^c \,. \tag{2}$$

Where n_i^c is the unit vector component describing the contact normal orientation. Components of this vector are related to the spherical coordinate system (Fig. 1) and are defined as

$$n_1^c = \cos\beta\sin\gamma\,,\; n_2^c = \sin\beta\sin\gamma\,,\; n_3^c = \cos\gamma\,. \tag{3}$$

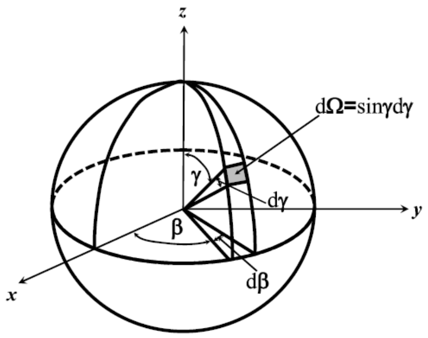

Figure 1. Illustration of three-dimensional vector

A particle pack may show anisotropy. The anisotropy may be classified in inherent, induced and initial. The inherent anisotropy is a consequence of the depositional processes. The geometry of particles influences this kind of anisotropy. As discussed by Oda (1972), it happens even when spherical ones are used (Oda, 1972). So, we consider that anisotropy needs to be determined.

It is possible and conceptually easy to relate the anisotropy to preferential orientation of the particles in the material. Orientations can be depicted using a probability density function $E\;\boldsymbol{n}$ where $\boldsymbol{n}$ is the unit vector that describes an orientation.

A good approximation of the contact orientation distribution is

$$\begin{cases} E(\boldsymbol{n}) = \dfrac{1}{4\pi}\left(1 + a_{ij}^{r} n_i^{c} n_j^{c}\right) \\ a_{ij}^{r} = a_{ji}^{r}, \quad a_{ii}^{r} = 0 \end{cases}, \tag{4}$$

where a_{ij}^{r} is the tensor of anisotropy, given by

$$a_{ij}^{r} = \frac{15}{2} R_{ij}^{'} . \tag{5}$$

Where $R_{ij}^{'}$ is the deviator fabric tensor and can be expressed as

$$R_{ij}^{'} = R_{ij} - \frac{\delta_{ij}}{3} . \tag{6}$$

If the distribution is uniform and isotropic, $E(\boldsymbol{n}) = 1/4\pi$ and $a_{ij}^{r} = 0$.

Similarly, distribution of average normal contact force $\bar{f}^{n}(\Omega)$ is given as

$$\begin{cases} \bar{f}^{n}(\Omega) = \bar{f}^{0}\left(1 + a_{ij}^{n} n_i n_j\right) \\ a_{ij}^{n} = a_{ji}^{n}, \quad a_{ii}^{n} = 0 \end{cases}, \tag{7}$$

where $\bar{f}^{0}$ symbolizes the normal contact force average over groups of orientation (these groups are given an equal weight) and it is defined as

$$\bar{f}^{0} = \frac{1}{4\pi} \int_{\Omega} \bar{f}^{n}(\Omega)\, d\Omega . \tag{8}$$

By analogy to fabric tensor, normal contact force tensor is given as

$$F_{ij}^{n} = \frac{1}{4\pi} \sum \bar{f}^{n}(\Omega^{g})\left(n_i n_j \Delta\Omega^{g}\right), \tag{9}$$

where Ω^{g} is a partitioned group of unit sphere.

The normal force anisotropy tensor is expressed as

$$a_{ij}^{n} = \frac{15}{2} F_{ij}^{'n} , \tag{10}$$

where

$$F_{ij}^{'n} = F_{ij}^{n} - \frac{\bar{f}^{0}}{3} . \tag{11}$$

Distribution of average tangential contact force $\bar{f}^{t}(\Omega)$ is given as

$$\begin{cases} \bar{f}^{t}(\Omega) = \bar{f}^{0}\left[a_{ij}^{t} n_j - \left(a_{kl}^{t} n_k n_l\right) n_i\right] \\ a_{ij}^{t} = a_{ji}^{t}, \quad a_{ii}^{t} = 0 \end{cases}. \tag{12}$$

We want to highlight that the contact force vector is the decomposed as the sum of a normal and tangential components. So, tangential contact force contribution could be calculated.

Tangential contact force tensor is given as

$$F_{ij}^{t} = \frac{1}{4\pi}\sum_{N^g} \bar{f}_i^{t} \;\; \Omega^g \;\; n_j \Delta\Omega^g \,. \tag{13}$$

Tangential contact force anisotropy tensor is

$$a_{ij}^{t} = 5\frac{F_{ij}^{t}}{\bar{f}^{0}} \,. \tag{14}$$

3.1 Fabric tensor using eigenvalue analysis

The fabric tensor is difficult to "visualize" and recognizing the similarity with stress tensor may be the best place to start an analysis (O'Sullivan, 2011).The principal stresses and their orientation can be determined from stress tensor. Similarly, the preferred orientations and the magnitude of the anisotropy can be determined from known fabric tensor. The method to measure the magnitude of anisotropy is not yet completely developed. However, researches tend to apply the eigenvalues. In this work, we define that Φ_1 is the major fabric, Φ_2 is the intermediate fabric and Φ_3 is the minor fabric directions.

In three dimensions, a fully anisotropic fabric will be characterized by three distinct eigenvalues. A transversely anisotropic one will be described by two distinct eigenvalues.

For two-dimensional systems, Table 1 shows different equations to quantify the anisotropy.

Table 1. Two-dimensional systems: equations to quantify the anisotropy

Researchers	Anisotropy
Curray (1956)	$\frac{\Phi_1 - \Phi_3}{2}$
Thornton (2000)	$\Phi_1 - \Phi_3$
Ibraim et al. (2006)	$\frac{\Phi_1}{\Phi_2}$
Maeda (2009)	$Z \;\; \Phi_1 - \Phi_3$

Interpretation of anisotropy in three-dimensional systems becomes more complicated. The quantification of anisotropy proposed by Barreto (2009) is

$$\Phi_d = \frac{1}{\sqrt{2}}\sqrt{\;\; \Phi_1 - \Phi_2 \;\;^{2} + \;\; \Phi_2 - \Phi_3 \;\;^{2} + \;\; \Phi_3 - \Phi_1 \;\;^{2}} \,. \tag{15}$$

O'Sullivan(2011) highlighted that Kuo et al. used a similar expression in 1998.

3.2 Coordination number and void ratio

As said above, the coordination number Z is a numerical mean of number of contacts for a particle in a pack. Additionally, Z is related to the density of a granular pack. During the analysis of regular arrangements of identical spheres, a strong correlation between Z and the avoid ratio (e) was identified (Cambou et al., 2009). So, various empirical formulae for irregular arrangements of particles were derived. The first one was written by Field in 1963:

$$Z = \frac{12}{1+e}. \tag{16}$$

The second empirical formulae was written by Athanasiou-Grivas and Harr in 1982:

$$Z = \frac{3}{e}\left(1+e\right). \tag{17}$$

The third empirical formulae was written by Yanagisawa in 1983:

$$Z = 3.183^{\,2.469-e}. \tag{18}$$

The last one was written by Chang, Misra and Sundararam in 1990:

$$Z = 13.28 - 8e. \tag{19}$$

These equations are used in the next section to calculate the coordination number for granular packs.

4 EXAMPLES

We employed our technique to generate multiple granular packs of both 2D and 3D bulk shapes. We adopted a gravity force of magnitude g as the jamming pseudo force and considered some energy dissipation. This jamming pseudo force acts in the direction from top to bottom of the bulk domain. The following data are common for all examples: Mass density of the particles = 1000 kg/m3; Elasticity modulus and Poisson coefficient of the particles (needed to resolve contacts/collisions with our DEM solver): $E = 10^8$ N/m² and $\nu = 0.25$; Damping rate for contacts/collisions: $\xi = 0.1$; Coefficient of dynamic friction for contacts/collisions: $\mu_d = 0.2$; Magnitude of gravity force (jamming pseudo-force): $g = 2$ m/s²; Drag force constant: $c_D = 0.005$ N·s/m; Initial velocity and spin of each newly generated particle: $\boldsymbol{v}(0) = \boldsymbol{w}_i(0) = \boldsymbol{o}$; Time step size for the DEM simulations: $\Delta t = 0.0001$ s; Duration of the jamming stage for each newly generated layer (i.e., DEM simulation time): $t = 1.0$ s; Typical number of particles in a pack: $N_p = 1300$ (2D packs) and $N_p = 7500 \sim 8000$ (3D packs). More detailed information about the particle generation process can be found in Campello and Cassares (2015).

4.1 2D rectangular packs of congruent particles

In this example, rectangular packs are considered and these have length $L = 1.0$ m and height desired $H_d = 0.5$ m. We adopted $r_i = 0.01$ m ($i = 1,\ldots,N_p$) for all particles. The initial thickness of each layer is set to $h_{layer} = 0.2H_d$ and the initial packing ratio is $\bar{\phi} = 0.4$. Using these data, ten packs are generated by means of Algorithm 1. We show the results in Fig. 2; the corresponding final densities are depicted in Table 2 and the coordination number calculated by means of Eq.16, Eq.17, Eq.18 and Eq.19 in Table 3. We repeat the procedure and generate another ten packs but now not considering rotational motion during the simulations of compaction stages. The results are shown in Fig. 3, the final densities are depicted in Table 2 and the coordination numbers are shown in Table 4.

Table 2. Packing densities (ϕ) obtained for example 4.1

Pack	rotations ON	rotations OFF
1	0.854	0.813
2	0.854	0.838
3	0.854	0.841
4	0.863	0.830
5	0.854	0.838
6	0.864	0.837
7	0.853	0.840
8	0.863	0.839
9	0.892	0.846
10	0.862	0.846
mean	0.861	0.837
st. deviation	0.012	0.010
coef. variation	0.014	0.012

Table 3. Packing coordination number (Z) obtained for example 4.1 (rotations ON)

Pack	e	Z -Fie(1963)	Z -Ath(1982)	Z -Yan(1983)	Z -Cha(1990)
1	0.171	10.248	20.544	14.306	11.912
2	0.171	10.248	20.544	14.306	11.912
3	0.171	10.248	20.544	14.306	11.912
4	0.159	10.354	21.868	14.506	12.008
5	0.171	10.248	20.544	14.306	11.912
6	0.158	10.363	21.987	14.523	12.016
7	0.172	10.239	20.442	14.290	11.904
8	0.158	10.363	21.987	14.523	12.016
9	0.122	10.695	27.590	15.141	12.304
10	0.16	10.345	21.750	14.489	12.000

Table 4. Packing coordination number (Z) obtained for example 4.1 (rotations OFF)

Pack	e	Z -Fie(1963)	Z -Ath(1982)	Z -Yan(1983)	Z -Cha(1990)
1	0.230	9.756	16.044	13.361	11.440
2	0.194	10.050	18.464	13.930	11.728
3	0.190	10.084	18.790	13.995	11.760
4	0.205	9.959	17.634	13.754	11.640
5	0.193	10.059	18.544	13.946	11.736
6	0.194	10.050	18.464	13.930	11.728
7	0.191	10.076	18.707	13.979	11.752
8	0.191	10.076	18.707	13.979	11.752
9	0.182	10.152	19.484	14.125	11.824
10	0.182	10.152	19.484	14.125	11.824

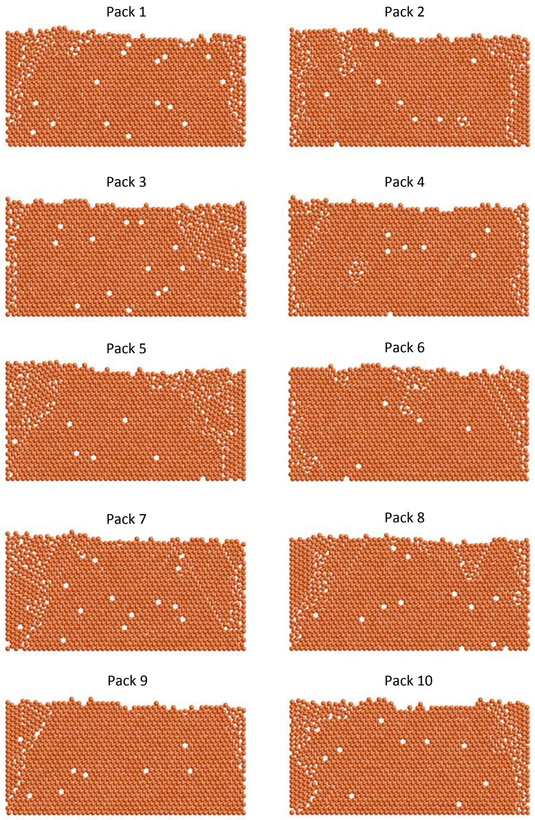

Figure 2. 2D packs of congruent particles (rotational motion is ON)

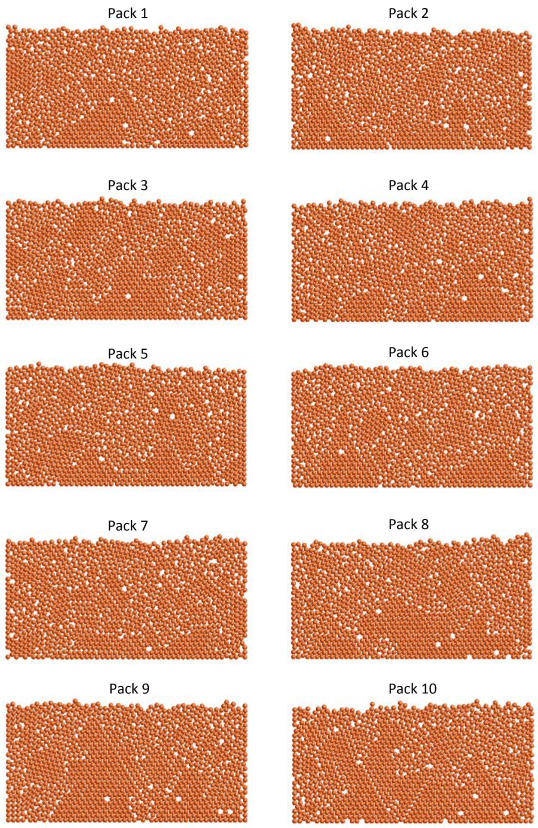

Figure 3. 2D packs of congruent particles (rotational motion is OFF)

4.2 2D rectangular packs of inhomogeneous particles

In this example we repeat the input data of the previous example but now generate packs of inhomogeneous particles. The particles´ radii are enforced to follow a Gaussian distribution of mean $r_m = 0.01\,\mathrm{m}$ and standard deviation $\sigma_r = 0.1 r_m$ m. The truncation limits of the distribution are set to $r_{min} = r_m - 3\sigma_r = 0.07\,\mathrm{m}$ and $r_{\max} = r_m + 3\sigma_r = 0.013\,\mathrm{m}$, which encompass more than 99% of the distribution. The results obtained with consideration of rotational motion are depicted in Fig. 4, whereas the ones for inhibited rotations are shown in Fig. 5. Table 5 summarizes the attained densities for both cases. The previous coordination numbers are shown in Table 6 and Table 7.

Table 5. Packing densities (ϕ) obtained for example 4.2

Pack	rotations ON	rotations OFF
1	0.826	0.803
2	0.830	0.827
3	0.825	0.814
4	0.819	0.815
5	0.822	0.814
6	0.825	0.819
7	0.826	0.813
8	0.822	0.810
9	0.827	0.806
10	0.826	0.806
mean	0.825	0.813
st. deviation	0.003	0.007
coef. variation	0.004	0.009

Table 6. Packing coordination number (Z) obtained for example 4.2 (rotations ON)

Pack	e	Z -Fie(1963)	Z -Ath(1982)	Z -Yan(1983)	Z -Cha(1990)
1	0.211	9.909	17.218	13.659	11.592
2	0.205	9.959	17.634	13.754	11.640
3	0.212	9.901	17.151	13.643	11.584
4	0.22	9.836	16.636	13.517	11.520
5	0.216	9.868	16.889	13.580	11.552
6	0.213	9.893	17.085	13.627	11.576
7	0.211	9.909	17.218	13.659	11.592
8	0.216	9.868	16.889	13.580	11.552
9	0.209	9.926	17.354	13.690	11.608
10	0.21	9.917	17.286	13.674	11.600

Table 7. Packing coordination number (Z) obtained for example 4.2 (rotations OFF)

Pack	e	Z -Fie(1963)	Z -Ath(1982)	Z -Yan(1983)	Z -Cha(1990)
1	0.246	9.631	15.195	13.116	11.312
2	0.209	9.926	17.354	13.690	11.608
3	0.229	9.764	16.100	13.377	11.448
4	0.227	9.780	16.216	13.408	11.464
5	0.228	9.772	16.158	13.392	11.456
6	0.221	9.828	16.575	13.501	11.512
7	0.231	9.748	15.987	13.346	11.432
8	0.235	9.717	15.766	13.284	11.400
9	0.24	9.677	15.500	13.208	11.360
10	0.241	9.670	15.448	13.192	11.352

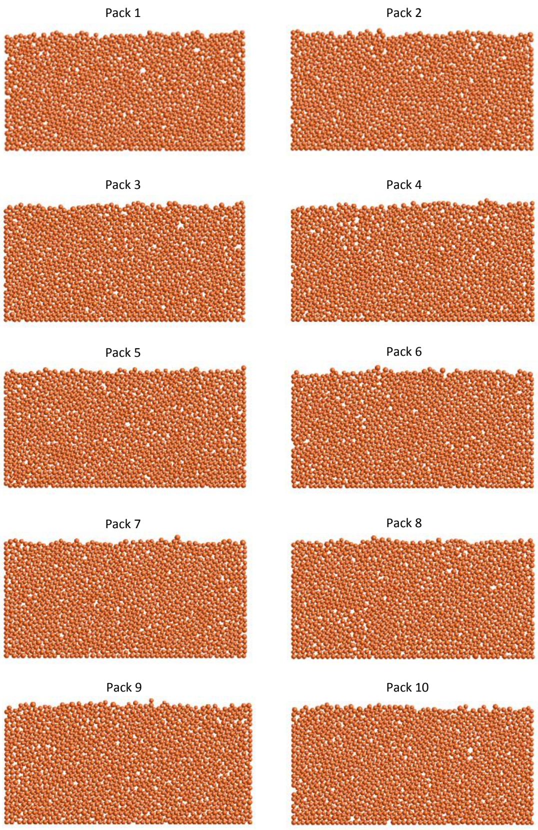

Figure 4. 2D packs of inhomogeneous particles (rotational motion is ON)

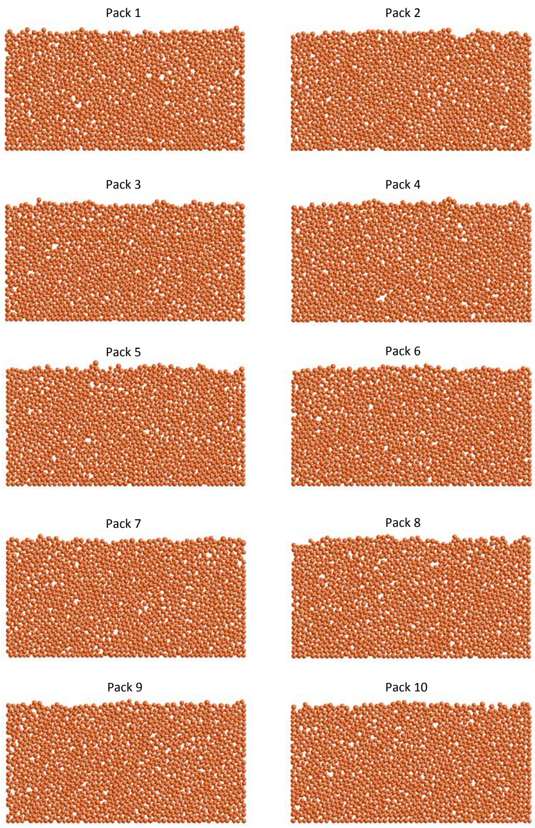

Figure 5. 2D packs of inhomogeneous particles (rotational motion is OFF)

4.3 3D brick packs of congruent particles

This is the three-dimensional version of example 4.1. We did some slightly modified data to keep the total number of particles in a pack not too large. Accordingly, the packs have a rectangular brick shape with horizontal base lengths $B_1 = B_2 = 1.0$ m and desired height $H_d = 0.5\,\text{m}$. Congruent particles of radius $r_i = 0.02\,\text{m}$ $(i = 1,\ldots,N_p)$ are considered to generate the packs. The initial thickness of each layer is $h_{layer} = 0.2H_d$ and the initial packing density is set to $\bar{\phi} = 0.25$. The results obtained with consideration of rotational motion are depicted in Fig. 6, whereas the ones for inhibited rotations are shown in Fig. 7. Table 8 summarizes the attained densities for both cases. The previous coordination numbers are shown in Table 9 and Table 10.

Table 8. Packing densities (ϕ) obtained for example 4.3

Pack	rotations ON	rotations OFF
1	0.560	0.540
2	0.576	0.538
3	0.572	0.539
4	0.608	0.542
5	0.564	0.534
6	0.559	0.541
7	0.563	0.539
8	0.560	0.540
9	0.564	0.539
10	0.561	0.536
mean	0.569	0.539
st. deviation	0.015	0.002
coef. variation	0.026	0.004

Table 9. Packing coordination number (Z) obtained for example 4.3 (rotations ON)

Pack	e	Z-Fie(1963)	Z-Ath(1982)	Z-Yan(1983)	Z-Cha(1990)
1	0.787	6.715	6.812	7.011	6.984
2	0.735	6.916	7.082	7.446	7.400
3	0.747	6.869	7.016	7.343	7.304
4	0.645	7.295	7.651	8.264	8.120
5	0.772	6.772	6.886	7.134	7.104
6	0.788	6.711	6.807	7.003	6.976
7	0.776	6.757	6.866	7.101	7.072
8	0.787	6.715	6.812	7.0109	6.984
9	0.772	6.772	6.886	7.134	7.104
10	0.783	6.730	6.831	7.043	7.016

Table 10. Packing coordination number (Z) obtained for example 4.3 (rotations OFF)

Pack	e	Z-Fie(1963)	Z-Ath(1982)	Z-Yan(1983)	Z-Cha(1990)
1	0.853	6.476	6.517	6.495	6.456
2	0.857	6.462	6.501	6.465	6.424
3	0.856	6.466	6.505	6.473	6.432
4	0.846	6.501	6.546	6.548	6.512
5	0.873	6.407	6.436	6.346	6.296
6	0.849	6.490	6.534	6.525	6.488
7	0.855	6.469	6.509	6.480	6.440
8	0.851	6.483	6.525	6.510	6.472
9	0.856	6.466	6.505	6.473	6.432
10	0.864	6.438	6.472	6.413	6.368

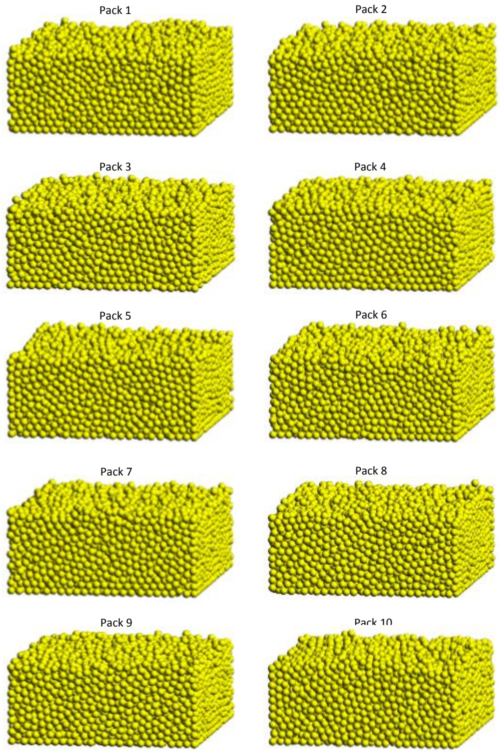

Figure 6. 3D packs of congruent particles (rotational motion is ON)

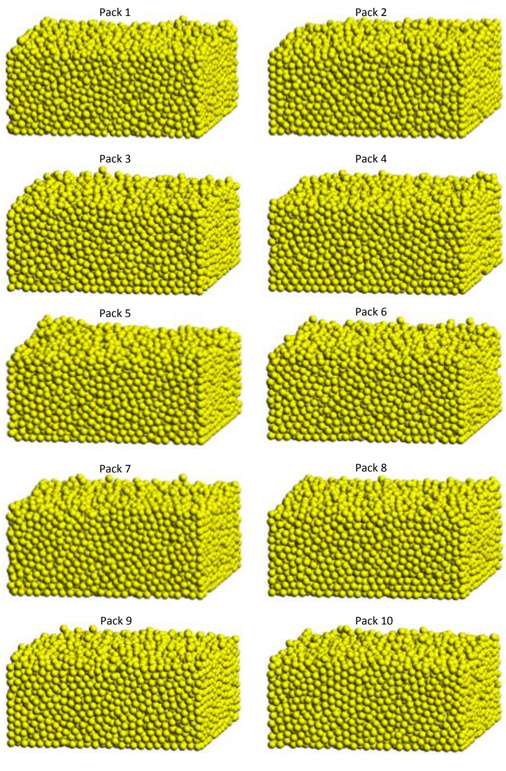

Figure 7. 3D packs of congruent particles (rotational motion is OFF)

4.4 3D brick packs of inhomogeneous particles

We consider the same data of the previous example, except that the packs are now generated with inhomogeneous particles. The particles´ radii follow a Gaussian distribution with mean $r_m = 0.02\,\mathrm{m}$, standard deviation $\sigma_r = 0.1 r_m\,\mathrm{m}$ and truncation limits $r_{\min} = r_m - 3\sigma_r = 0.014\,\mathrm{m}$ and $r_{\max} = r_m + 3\sigma_r = 0.026\,\mathrm{m}$ (this encompasses more than 99% of the distribution). The results obtained are depicted in Fig. 8 (with consideration of rotational motion) and Fig. 9 (for inhibited rotations). Table 11 summarizes the attained densities for both cases. . The previous coordination numbers are shown in Table 12 and Table 13.

Table 11. Packing densities (ϕ) obtained for example 4.4

Pack	rotations ON	rotations OFF
1	0.578	0.548
2	0.563	0.543
3	0.566	0.552
4	0.571	0.547
5	0.567	0.542
6	0.574	0.552
7	0.578	0.553
8	0.575	0.542
9	0.578	0.546
10	0.578	0.538
mean	0.573	0.546
st. deviation	0.006	0.005
coef. variation	0.010	0.009

Table 12. Packing coordination number (Z) obtained for example 4.4 (rotations ON)

Pack	e	Z -Fie(1963)	Z -Ath(1982)	Z -Yan(1983)	Z -Cha(1990)
1	0.732	6.928	7.098	7.472	7.424
2	0.776	6.757	6.866	7.101	7.072
3	0.768	6.787	6.906	7.167	7.136
4	0.752	6.849	6.989	7.301	7.264
5	0.764	6.803	6.927	7.200	7.168
6	0.744	6.881	7.032	7.369	7.328
7	0.732	6.928	7.098	7.472	7.424
8	0.74	6.897	7.054	7.403	7.360
9	0.732	6.928	7.098	7.472	7.424
10	0.732	6.928	7.098	7.472	7.424

Table 13. Packing coordination number (Z) obtained for example 4.4 (rotations OFF)

Pack	e	Z -Fie(1963)	Z -Ath(1982)	Z -Yan(1983)	Z -Cha(1990)
1	0.824	6.579	6.641	6.717	6.688
2	0.843	6.511	6.559	6.571	6.536
3	0.812	6.623	6.695	6.811	6.784
4	0.827	6.568	6.628	6.694	6.664
5	0.843	6.511	6.559	6.571	6.536
6	0.812	6.623	6.695	6.811	6.784
7	0.807	6.641	6.718	6.850	6.824
8	0.844	6.508	6.555	6.563	6.528
9	0.832	6.550	6.606	6.655	6.624
10	0.86	6.452	6.488	6.443	6.400

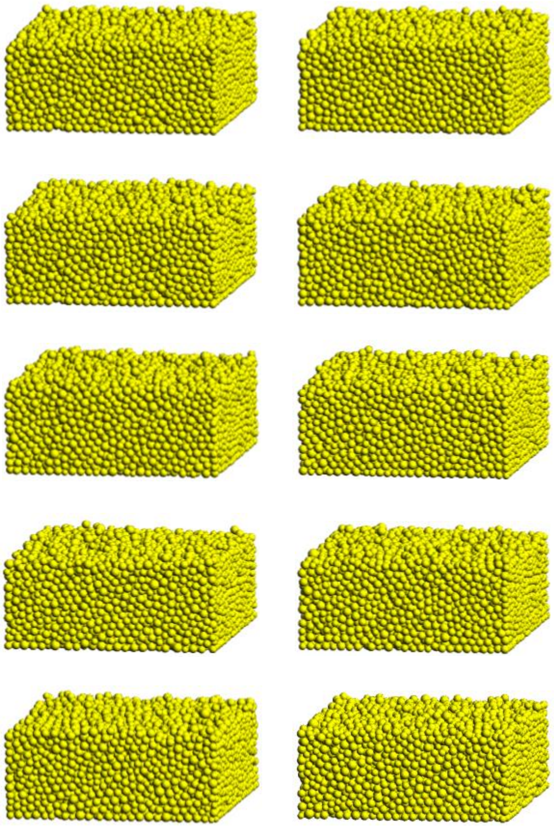

Figure 8. 3D packs of inhomogeneous particles (rotational motion is ON)

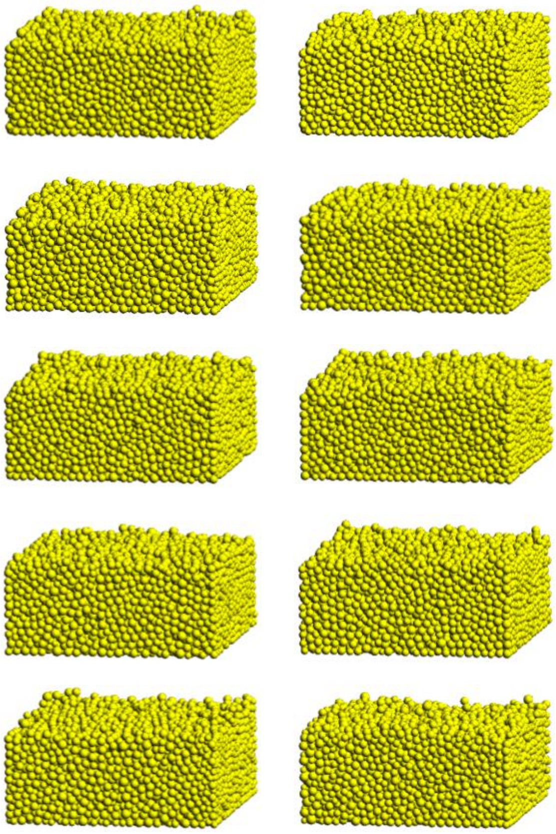

Figure 9. 3D packs of inhomogeneous particles (rotational motion is OFF)

CONCLUSIONS

This work is a preliminary study about the fabric of 2D and 3D packs generated with our recently proposed packing generation algorithm. We want to highlight that these packs of spherical particles were generated using a technique that, though very simple and fast, allows adequately high packing densities and more or less repeatable (yet randomly generated) fabrics or microstructures. This feature is extremely desirable if the packs are intended to serve as samples of granular materials on which DEM simulations are to be conducted, e.g. for material characterization purposes and/or determination of bulk material responses. This is indeed our interest in the next step of this research.

ACKNOWLEDGEMENTS

This work was supported by CNPq (Conselho Nacional de Desenvolvimento Científico e Tecnológico) and FAPESP (São Paulo State Science Foundation) under the grants 303793/2012-0 and 2014/19821-7. respectively.

REFERENCES

Bathrust, R. J., 1985. *A study of stress and anisotropy in idealized granular assemblies*. PhD thesis, Queen’s University/Canada.

Cambou, B. et al., 2009. *Micromechanics of granular materials*. ISTE and John Wiley & Sons.

Campello, E. M. B., Cassares, K. R., 2015 (submitted). Rapid generation of particle packs at high packing ratios for DEM simulations of granular compacts. *Lat. Amer. J. Sol. Struct.*

Chang, C. S., Chao, S. J., & Chang, Y., 1995. Estimates of elastic moduli fir granular material with anisotropic random packing structure. *Int. J. Solid and Struct.*, vol. 32, n. 4, pp. 1989–2008.

Cundall, P. A., & Strack, O. L., 1979. A discrete numerical model for granular assemblies. *Géotechnique*, vol. 29, n. 1, pp. 47–65.

Cundall, P. A. et al., 1982. Numerical experiments on granular assemblies; measurements and observations. In Vermeer, P. A., Luger, H. J., eds, *Deformation and Failure of Granular Materials*, pp. 355–370. Balkema, Rotterdam.

Darbre, G. R., & Wolf, J. P., 1985. Nonlinear elastic constitutive law for granular materials applicable to pebble-bed core. *Nuclear Engineering and Design*, vol. 88, n. 2, pp. 161–168.

Emeriault, F., & Cambou, B., 1996. Micromechanical modelling of anisotropic non-linear elasticity of granular medium. *Int. J. Solids Structures*, vol. 33, n. 18, pp. 2591–2607.

Kruyt, N. P., 2012. Micromechanical study of fabric evolution in quasi-static deformation of granular materials. *Mechanics of Materials*, vol. 44, pp. 120–129.

Ng, T.-T., 1999. Fabric study of granular materials after compaction. *Journal of Engineering Mechanics*, vol. 125, n. 12, pp. 1309–1394.

Ng, T.-T., 2001. Fabric evolution of ellipsoidal arrays with different particle shapes. *Journal of Engineering Mechanics*, vol. 127, n. 10, pp. 994–999.

Ng, T.-T., 2004. Macro- and micro-behaviors of granular materials under different sample preparation methods and stress paths. *Int. J. Solid and Struct.*, vol. 41, n. 21, pp. 5871–5884.

Oda, M., 1972. The mechanism of fabric changes during compressional deformation of sand. *Soils and Found.*, vol. 12, n. 2, pp. 1–18.

O'Sullivan, C., 2011. *Particulate discrete element modelling – A geomechanics perspective*. Spon Press.

Rothenburg, L., 1980. *Micromechanics of idealized granular systems*. PhD thesis, Carleton University/Canada.

Rothenburg, L., & Bathrust, R. J., 1989. Analytical study of induced anisotropy in idealized granular materials. *Géotechnique*, vol. 39, n. 4, pp. 601–614.

Rothenburg, L., & Bathrust, R. J., 1992. Micromechanical features of granular assemblies with planar elliptical particles. *Géotechnique*, vol. 42, n. 2, pp. 79–95.

Rothenburg, L.; & Kruyt, N. P., 2004. Critical state and evolution of coordination number in simulated granular materials. *International Journal of Solids and Structure*, vol. 41, n. 21, pp. 5763–5774.

Shertzer, R. H., 2011. *Fabric tensors and effective properties of granular materials with application to snow*. PhD thesis, Montana State University/Montana.

Thornton, C., & Barnes, D. J., 1986. Computer Simulated Deformation of Compact Granular Assemblies. *Acta Mechanica*, vol. 64, n. 1-2, pp. 45–61.

Thornton, C.; & Antony, S. J., 1998. Quasi-static deformation of particulate media. *Phil. Trans. R. Soc. Lond A*, n. 356, n. 1747, pp. 2763–2782.

Thornton, C., 2000. Numerical simulations of deviatoric shear deformation of granular media. *Géotechnique*, n. 50, n. 1, p. 43–53.